Oncogene (2013), 1–11

www.nature.com/onc

ORIGINAL ARTICLE

c-Myc and Her2 cooperate to drive a stem-like phenotype with poor prognosis in breast cancer

R Nair[1], DL Roden[1], WS Teo[1,2], A McFarland[1], S Junankar[1,2], S Ye[1,2], A Nguyen[1], J Yang[1], I Nikolic[1], M Hui[1], A Morey[2,3], J Shah[4], AD Pfefferle[5,6], J Usary[6,7], C Selinger[8], LA Baker[1,9], N Armstrong[10], MJ Cowley[1,11], MJ Naylor[1,2,12], CJ Ormandy[1,2], SR Lakhani[13], JI Herschkowitz[14], CM Perou[5,6,7], W Kaplan[2,11], SA O'Toole[1,2,8,15] and A Swarbrick[1,2]

The *HER2* (*ERBB2*) and *MYC* genes are commonly amplified in breast cancer, yet little is known about their molecular and clinical interaction. Using a novel chimeric mammary transgenic approach and *in vitro* models, we demonstrate markedly increased self-renewal and tumour-propagating capability of cells transformed with Her2 and c-Myc. Coexpression of both oncoproteins in cultured cells led to the activation of a c-Myc transcriptional signature and acquisition of a self-renewing phenotype independent of an epithelial–mesenchymal transition programme or regulation of conventional cancer stem cell markers. Instead, Her2 and c-Myc cooperated to induce the expression of lipoprotein lipase, which was required for proliferation and self-renewal *in vitro*. *HER2* and *MYC* were frequently coamplified in breast cancer, associated with aggressive clinical behaviour and poor outcome. Lastly, we show that in *HER2*$^+$ breast cancer patients receiving adjuvant chemotherapy (but not targeted anti-Her2 therapy), *MYC* amplification is associated with a poor outcome. These findings demonstrate the importance of molecular and cellular context in oncogenic transformation and acquisition of a malignant stem-like phenotype and have diagnostic and therapeutic consequences for the clinical management of *HER2*$^+$ breast cancer.

Oncogene (2013) advance online publication, 23 September 2013; doi:10.1038/onc.2013.368

Keywords: Her2; *ERBB2*; Myc; cancer stem cell; transcriptomics; oncogene cooperation

INTRODUCTION

Despite dramatic advances in the clinical management of breast cancer over the past 20 years, treatment of breast cancer remains a major clinical challenge worldwide, with more than 400 000 women estimated to die from breast cancer each year.[1,2] Approximately 15–20% of breast cancers have amplification of *HER2* (*HER2*$^+$), with up to 25–50 copies of the gene per cell that is associated with a relatively poor prognosis.[3–5] c-Myc is a member of the basic helix–loop–helix transcription factor family and is amplified in many malignancies including in ~12–18% of breast cancers.[6–10] Intriguingly, several studies have reported that many *MYC*-amplified breast cancers also harbour *HER2* amplification, suggesting a selection for coamplification.[11,12] c-Myc cooperates in transformation with the activation of a variety of kinase signalling pathways and was identified as a downstream target of Her2-phosphatidylinositol 3-kinase signalling more than a decade ago.[13] Yet, despite being two of the most commonly amplified genes in breast cancer, little is known about the interaction of Her2 and c-Myc in breast cancer aetiology or the impact of *MYC* amplification on the *HER2*$^+$ cancer phenotype.[13–15] In this work, we demonstrate a potent interaction between Her2 and c-Myc, which drives mammary oncogenesis. Using mouse models and *in vitro* assays, we demonstrate that transformation with Her2 and c-Myc is sufficient to impart high self-renewal and tumour-propagating capacity. Transcriptomic analysis revealed that Her2 potentiates the expression of Myc target genes, specifically lipoprotein lipase (LPL), indicating the essential role for LPL in self-renewal in the context of cancer cell survival. Analysis of a clinical cohort validated that coamplification of *HER2* and *MYC* is common in breast cancer and associates with poor prognosis. Importantly, we also find that *MYC* amplification correlates with poor prognosis in *HER2*$^+$ patients receiving adjuvant chemotherapy. Thus, our studies reveal a role for Her2 and c-Myc cooperation in the development of aggressive tumours with high self-renewal and tumour-propagating characteristics.

RESULTS

Generation of mouse tumour models to study the interaction of Her2 and c-Myc

To experimentally test the interaction of Her2 and c-Myc activation *in vivo*, we used a chimeric mouse transgenic method,

[1]Cancer Research Division, The Kinghorn Cancer Centre and Cancer Research Program Garvan Institute of Medical Research, Darlinghurst, NSW, Australia; [2]St Vincent's Clinical School, Faculty of Medicine, University of New South Wales, Sydney, NSW, Australia; [3]Department of Anatomical Pathology, Sydpath, St Vincent's Hospital, Darlinghurst, NSW, Australia; [4]School of Medical Sciences, University of New South Wales, Camperdown, NSW, Australia; [5]Department of Pathology and Laboratory Medicine, Chapel Hill, NC, USA; [6]Lineberger Comprehensive Cancer Center, Chapel Hill, NC, USA; [7]Department of Genetics, University of North Carolina, Chapel Hill, NC, USA; [8]Department of Tissue Pathology and Diagnostic Oncology, Royal Prince Alfred Hospital, Camperdown, NSW, Australia; [9]School of Biotechnology and Biomolecular Sciences, University of New South Wales, NSW, Australia; [10]School of Mathematics and Statistics, The University of Sydney, Sydney, NSW, Australia; [11]Peter Wills Bioinformatics Centre, Garvan Institute of Medical Research, Darlinghurst, NSW, Australia; [12]Discipline of Physiology and Bosch Institute, School of Medical Sciences, University of Sydney, Sydney, NSW, Australia; [13]The University of Queensland, UQ Centre for Clinical Research, School of Medicine and Pathology Queensland, The Royal Brisbane and Women's Hospital, Herston, Brisbane, QLD, Australia; [14]Department of Molecular and Cellular Biology, Baylor College of Medicine, Houston, TX, USA and [15]Sydney Medical School, University of Sydney, Sydney, NSW, Australia. Correspondence: Dr A Swarbrick, Cancer Research Division, The Kinghorn Cancer Centre and Cancer Research Program Garvan Institute of Medical Research, 370 Victoria Street, Darlinghurst, NSW 2010, Australia.
E-mail: a.swarbrick@garvan.org.au
Received 27 February 2013; revised 23 July 2013; accepted 26 July 2013

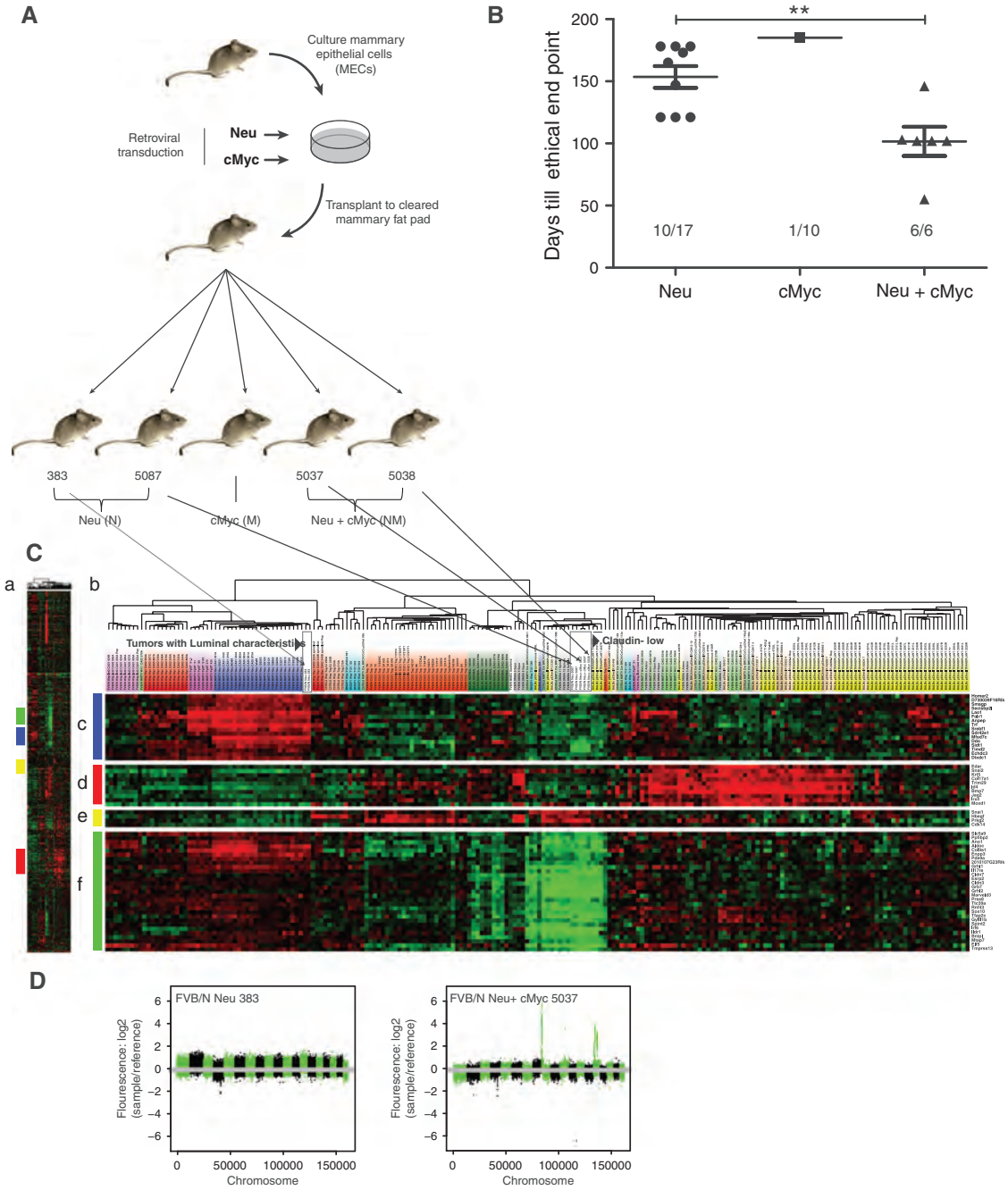

Figure 1. *In vivo* modelling of Her2 and c-Myc interaction. (**A**) Schematic showing the generation of tumour clones used to study the interaction between Her2 and c-Myc in breast cancer. Two independent tumour clones overexpressing Neu and Neu + c-Myc and one c-Myc tumour were used for further analysis. The clone numbers in the schematic are used in later figures. (**B**) Cooperation of Her2 and c-Myc in tumourigenesis *in vivo*. Only 10 in 17 Neu- and 1 in 10 c-Myc-overexpressing MECs transplanted into mice developed tumours, whereas Neu cooperated with c-Myc to drive the development of tumours with 100% penentrance (6/6). ***P*-value <0.01, *t*-test. (**C**) Mouse intrinsic gene set cluster analysis of our models with 117 samples from 13 GEMM (Genetically Engineered Mouse Model) previously published in Herschkowitz *et al.*[20] (**a**) Overview of the complete cluster diagram. (**b**) Experimental sample-associated dendogram, with boxes indicating our model subtypes based on SigClust analysis. Arrows indicate the tumour clone corresponding to tumour subtype. (**c**) Luminal epithelial gene expression pattern that is highly expressed in one of the FVB/N-Neu clones. (**d**) Basal epithelial expression patterns. (**e**) Mesenchymal genes, which are highly expressed in one of the Neu and both Neu + c-Myc tumours. (**f**) Genes expressed at low levels in claudin-low tumours. (**D**) Array CGH profiles of a representative Neu and Neu + c-Myc tumour showing increased genomic instability in the Neu- and c-Myc-overexpressing tumours. Each dot represents the average log 2 ratio of the sample/reference fluorescence of a DNA probe (Y axis) plotted at its genomic position (X axis). The alternating green and black colours denote separate individual chromosomes.

which has been successfully used previously to generate mammary-specific transgenics[15] (Figure 1A). The expression of the relevant oncogenes was confirmed by immunoblotting of extracts taken from transfected mammary epithelial cells (MECs) (Supplementary Figure 1D) before transplantation and from tumours that developed subsequently.

Only 1 of 10 c-Myc (M) transgenic mice developed a tumour, with a latency of 200 days.[15–17] The expression of a truncated

constitutively activated form of Neu (N),[18] the rodent homolog of Her2, alone generated tumours in 10 of 17 mice with a median tumour-free survival of 178 days, almost identical to the mouse mammary tumour virus-Neu transgenic mouse.[19] In contrast, c-Myc cooperated with Neu in tumourigenesis (NM), driving the early development of tumours with median tumour-free survival of 102 days and 100% penetrance (Figure 1B). Gene expression profiling for classification[20,21] revealed that the NM tumours clustered with the claudin-low subtype and were enriched in the expression of mesenchymal genes (Figure 1C (b, e)). Detailed characterization of the tumour models included array comparative genomic hybridization (CGH) analysis to determine copy number variants (Figure 1D). The NM tumours were more genomically unstable than N tumours, with a greater number of amplifications/deletions or rearrangements across multiple loci (Supplementary Table T6). One of the NM tumours (5037) had high amplification of *MYC*, which was reflected in high expression of c-Myc (Supplementary Figure 1D). Interestingly, the other NM tumour (5038) did not show any *c-Myc* amplification, but had high expression of Myc and Neu. Histopathological examination of tumours revealed that the retroviral Neu model developed luminal cytokeratin-positive (CK 8) adenocarcinomas, closely resembling those described in the mouse mammary tumour virus-Neu transgenic models[22] (Supplementary Figure 1C). The expression of c-Myc alone caused increased branching and hyperplastic lateral budding in all cases (data not shown), as previously described in transgenic and chimeric mouse models.[15–17] NM tumours were well defined and circumscribed with central necrosis and expressed the basal/myoepithelial markers cytokeratins 6 and 14.

Self-renewal capacity of NM tumours is greatly enhanced compared with those transformed by Neu alone

There is accumulating evidence that acquisition of a stem-like state is associated with a poor-prognosis phenotype in cancer.[23,24] c-Myc[7] and Her2[5] have both been implicated in the generation or maintenance of mammary stem and progenitor cells. We therefore asked whether NM tumours were enriched for self-renewal using serial passage in the 'tumoursphere' assay as shown in the schematic (Supplementary Figure 1A). In this assay, primary tumoursphere-forming capacity is indicative of short-term proliferative capacity, whereas sphere-forming capacity upon passage is proportional to self-renewal capacity. Although there was no difference between groups in primary sphere-forming capacity, NM tumour cells had an approximately eightfold enrichment in tumoursphere formation over those derived from N tumours after serial passage (Figures 2a and b). Interestingly, MECs transformed by Neu alone were not enriched for self-renewal when compared with control MECs. c-Myc alone generated tumours too rarely to

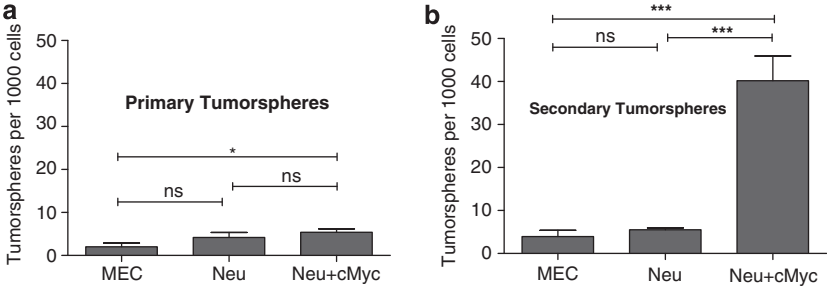

c

Tumor model/ Cell dilution	10,000	1000	100	10	Tumor Propagating Frequency
Neu					
383	3/3	2/3	1/5	-	1 in 743.74
5087	2/3	0/3	0/5	-	1 in 11002.85
383	3/3	2/3	1/3	-	1 in 669.54
Neu+c-Myc					
5037	-	3/3	3/3	4/5	1 in 6.21
5038	3/3	1/6	0/6	0/7	1 in 3807.96
5037	-	6/6	6/6	6/6	1 in 1

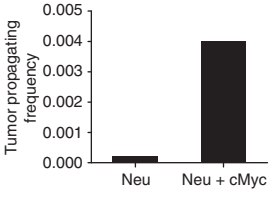

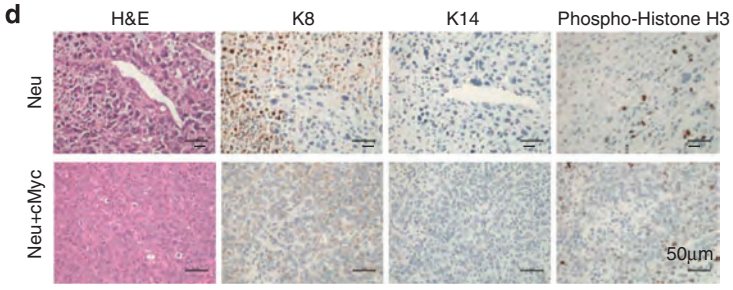

Figure 2. Neu and c-Myc cooperate to increase the self-renewal capacity of tumours. (**a**) Primary tumoursphere formation was not significantly different between MECs or tumour cells. **P*-value <0.05, *t*-test. (**b**) When passaged to secondary tumoursphere, tumour cells with Neu and c-Myc overexpression had eightfold increase in self-renewal capacity as compared with cells with single oncogene overexpression. ****P*-value <0.001, *t*-test. (**c**) Limiting dilution analysis to demonstrate *in vivo* self-renewal capacity of Neu and c-Myc interaction. The TPF of tumour cells overexpressing Neu and c-Myc was fourfold greater than Neu alone. (**d**) Analysis of cytokeratin and proliferative staining (phospho-histone H3) of tumours formed in Figure1a did not reveal any differences in proliferative ability. NS, nonsignificant.

be analysed. To determine the extent of self-renewal and *in vivo* tumour-propagating capacity of NM tumour cells, primary tumourspheres were passaged at clonal density into 96-well low attachment plates and wells containing single cells visually confirmed. Clonal tumourspheres were transplanted into syngeneic mice (Supplementary Figure 1A). All single tumourspheres rapidly generated palpable tumours *in vivo*, demonstrating extensive self-renewal and tumour-propagating capacity of even a single NM tumour cell.

We further confirmed the tumour-propagating frequency (TPF) of cells taken from each model using limiting dilution transplantation of tumour cells into syngeneic mice (Supplementary Figure 1B). N tumours cells contained rare tumour-propagating cells at an average frequency of $\sim$1 in 3907 cells, very similar to that reported previously in the mouse mammary tumour virus-Neu model (Figure 2c).[25,26] In stark contrast, the TPF of the NM tumour cells across all tumours was 1 in 212. In one clone, $<$10 cells were required for tumour propagation. Therefore, coexpression of Neu and c-Myc drives the rapid development of tumours with massive self-renewal potential and 20-fold enrichment in TPF compared with Neu on its own.

To determine the potency of these cells to differentiate and proliferate, we analysed the cytokeratin and proliferative staining pattern of tumours generated by the lowest cell dilution (Figure 2d and Supplementary Table T1). We did not observe any significant difference in the proliferative index (as determined by phosphohistone H3). This suggests that the aggressive phenotype observed by the cooperation of Her2 and c-Myc is not mainly driven by proliferation.

Her2 and c-Myc overexpression is sufficient for increased self-renewal

To determine whether Her2 and c-Myc overexpression alone is sufficient to impart this cancer stem cell (CSC) phenotype, we developed an *in vitro* model, based on the overexpression of c-Myc and Her2 in the MCF10A-immortalized breast epithelial cell line. Cell lines overexpressing full-length Her2 and c-Myc, singly or in combination—vector (V), Her2 (H), c-Myc (M) and Her2 + c-Myc (HM)—were generated and used to test the cooperative nature of their interaction. Overexpression of Her2 and c-Myc was confirmed by immunoblot (Figure 3a) in the appropriate modified cell lines. Interestingly, we found that the proliferation of the modified cell lines did not differ significantly (Supplementary Figure 2A), in agreement with the *in vivo* data (Figure 2d and Supplementary Table T1).

All cultures formed equivalent numbers of tumourspheres at the first passage (Supplementary Figure 2B); however, upon passage, HM cells formed a significantly higher number of tumourspheres when compared with control cells or those expressing either oncogene alone (Figure 3b). Thus, activation of c-Myc and Her2 is sufficient to impart increased self-renewal.

Her2 and c-Myc cooperation does not correlate with an EMT programme or the expression of CSC markers

To understand the molecular changes underpinning the acquisition of this CSC phenotype, we evaluated the effects of Her2 and c-Myc on known Her2 effector pathways and did not observe any significant changes in the phosphorylated forms of the Ras/mitogen-activated protein kinase or phosphatidylinositol 3-kinase/AKT pathway between the modified cell lines (data not shown).[13,14] c-Myc activity is regulated by phosphorylation on Thr58 and Ser62 by a number of kinases including GSK-3β [27] and Erk,[28] but there was a comparable increase in the p-c-MycT58 and p-c-MycS62 forms in both M- and HM-modified cell lines (Supplementary Figure 2C).

Previous data implicate the activation of an EMT programme by Her2 overexpression in the acquisition of a CSC-like phenotype[29] and we observed an increase in the TPF of NM tumours (Figure 2c). Consistent with previous reports, H cells had decreased levels of E-cadherin (an epithelial marker) and

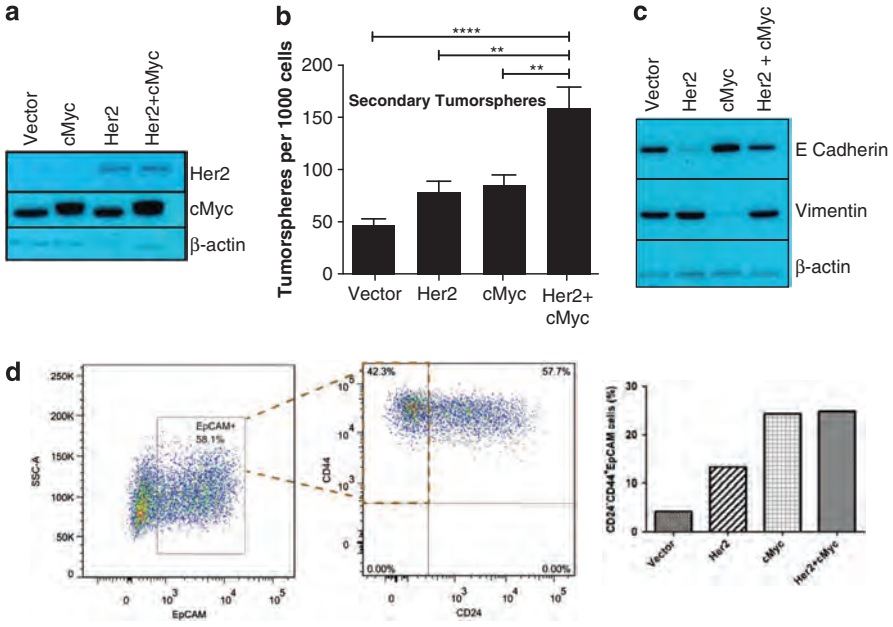

Figure 3. *In vitro* modelling of Her2 and c-Myc interaction. (**a**) Her2 and c-Myc overexpression in modified MCF10A cell lines determined by western blots. (**b**) Although the primary tumoursphere-forming capacity was not significantly different between the groups, Her2- and c-Myc-overexpressing cells have greater secondary tumoursphere-forming potential. ***P*-value $<$0.05, *****P*-value $<$0.0001, *t*-test. (**c**) The EMT programme is activated in Her2-overexpressing cells but not by c-Myc alone. HM cells on the other hand express both E-cadherin and vimentin. (**d**) Representative scatter plot from Her2- and c-Myc-overexpressing MCF10A cell lines and column graph showing the flow cytometry gating strategy used (left) to determine the CSC fraction marked by $CD24^-CD44^+EpCAM^+$ (right) in modified MCF10A cell lines. Overexpression of Her2, c-Myc or Her2 and c-Myc increased the CSC fraction to varying degrees but did not correlate with tumoursphere results in (**b**).

increased expression of vimentin (mesenchymal marker), whereas overexpression of c-Myc had the converse effect (Figure 3c). However, HM cells expressed both vimentin and E-cadherin at levels similar to those observed in control cells. This was supported by the expression of miR-200c, which is known to have a critical role in suppressing EMT[30,31] (Supplementary Figure 2D). In addition, we verified these observations by gene set enrichment analysis (GSEA) (as described in Materials and methods section) and demonstrate that two gene sets representative of EMT[32,33] (SARRIO_EPITHELIAL_MESENCHYMAL_TRANSITION_UP, ALONSO_METASTASIS_EMT_UP) (Supplementary Figure 2E) are both elevated in H cells, reduced in M cells and at levels similar to control in HM cells. Thus, it appears that Her2 and c-Myc cooperate to drive the acquisition of a self-renewing CSC phenotype through mechanisms distinct from the EMT programme.

We analysed the expression of a panel of commonly used CSC markers[34,35] in our cell line models.[36,37] We observed an approximately threefold increase in the CSC fraction in H compared with control cells (Figure 3d) as reported previously.[5] Myc overexpression led to an approximately sixfold increase in this cellular fraction, which was very similar to that seen in cultures overexpressing both oncogenes. When compared with the results of tumoursphere assays shown in Figure 3b, these data suggest that the CSC markers do not necessarily mark cells with greater self-renewal capacity. Similarly, expression of the murine CSC markers, CD29, CD24 and CD61,[38] did not correlate with self-renewal or TPF when we examined N and NM mouse tumours using flow cytometry (data not shown).

Transcriptional analysis of Her2 and c-Myc cooperation

We used transcriptomic analysis to explore the possibility that alterations in the c-Myc-dependent transcription programme underlie the cooperation between Her2 and c-Myc. We performed whole genome expression profiling to define data sets for MCF10A cells expressing H, M, HM or V. Limma analysis revealed unique and partially overlapping patterns of expression in each group, including eight genes that were uniquely upregulated and 18 downregulated in the HM signature (Supplementary Figure 3A). Genes of interest were selected for validation by quantitative real-time polymerase chain reaction (qRT-PCR) based on their unique expression in the HM data set and their potential functional role in breast cancer. There was more than a 14-fold increase in LPL levels compared with vector control (Figure 4a) in the HM group.

We used GSEA[39] to understand the functional and regulatory relationships between genes in the H, M and HM signatures. We systematically looked for gene sets that were enriched in the HM

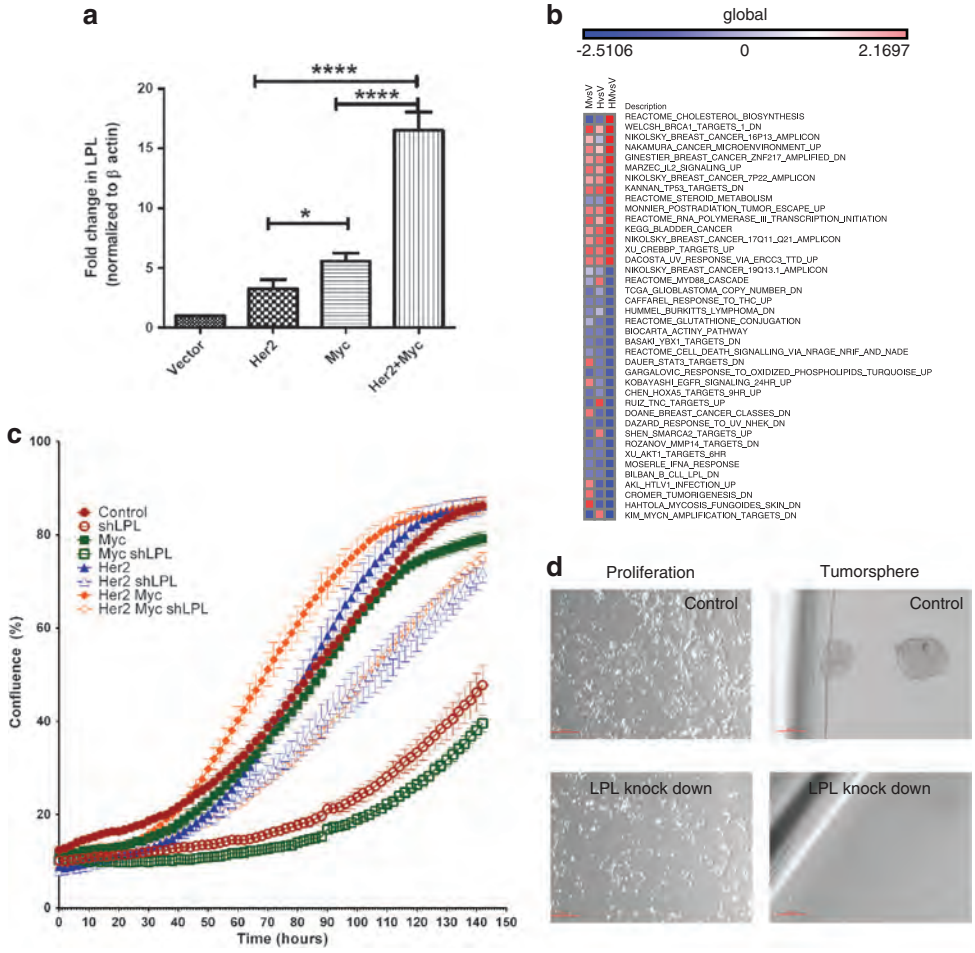

Figure 4. Transcript profiling reveals genes and enriched gene sets that drive the HM coexpressing poor prognosis phenotype. (**a**) LPL fold change as determined by qRT-PCR shows 14-fold increase in HM cells compared with vector control in three independent samples, **P*-value <0.05, *****P*-value <0.0001, *t*-test. (**b**) Gene sets (sorted by HMvsV NES values) identified as significantly enriched (false discovery rate <0.05) by GSEA in HM cells and also passed NES enrichment filters as described in Results section. (**c**) LPL knockdown leads to decrease in proliferative and tumoursphere-forming ability of all cell lines (number of biological replicates = 2). (**d**) Images are of cells in two- and three-dimensional tumoursphere formation of representative HM control and knockdown cells.

cells when compared with both the H or M cells. We first identified gene sets that were significantly enriched (i.e., q-value <0.05) in the HM cells. Using the GSEA normalized enrichment scores as a measure of relative enrichment between experiments, we next applied an additional filter to identify those gene sets that showed an increase in normalized enrichment score (NES), of 25% or more, between the most enriched single oncogenic expression signature and that observed from HM coexpression. Using this method, we identified gene sets in the Broad Institute's Molecular Signature Database (MSigDb; Subramanian *et al.*[39]) that were enriched in the HM signature when compared with the H or M signatures. We investigated the curated 'C2' gene sets, leading to the identification of 40 enriched gene sets (Figure 4b) encompassing a diversity of processes including a number of signatures associated with poor prognosis cancers.

Of interest, several gene sets involved in sterol and lipid biology (REACTOME_CHOLESTEROL_BIOSYNTHESIS and REACTOME_STEROID_METABOLISM) were significantly upregulated in the HM group (Figure 4b).[40] We also found a significant correlation between the HM gene signature and a poor prognosis gene expression signature previously associated with high expression of *LPL*, a gene involved in lipid utilization and cholesterol uptake. A set of genes (BILBAN_B_CLL_LPL-DN; Bilban *et al.*[41]) with reduced expression in tumours with high LPL (patients with poor prognosis) were also downregulated in the HM group (Figure 4b). To test whether LPL was important to the phenotype of these cells, we tested the impact of LPL depletion on proliferation and self-renewal. Surprisingly, depletion of LPL in all four cell lines led to a significant decrease in proliferation and tumoursphere formation (Figure 4c,d). Although cell lines transduced with control short hairpin RNA formed about five primary tumourspheres per 1000 cells, LPL knockdown led to a complete abrogation in tumoursphere formation of all the cell lines (Figure 4d), suggesting an important role for LPL in self-renewal or survival in suspension culture.

GSEA analysis also showed that genes that were significantly downregulated in *MYCN*-amplified cancer cells (KIM_MYCN_AMPLIFICATION_TARGETS_DN)[42] were also significantly downregulated in the M and HM cells (Figure 4b and Supplementary Figure 3B). However, Her2 and c-Myc (q-value of 0.0001) cooperated to downregulate the *MYCN* targets much more significantly than c-Myc (q-value of 0.01) overexpression alone, showing a 30% decrease in the GSEA NES for the HM cells. In addition, using the 'C3' transcription factor motif gene sets in GSEA, a significant upregulation ($q<0.05$) of genes enriched with MYC binding sites was seen for the HM-coexpressing cells but not in either of the H or M. These data suggest that coexpression with Her2 amplifies the expression of a set of Myc transcriptional targets.

Coamplification of *HER2* and *MYC* correlates with poor prognosis

To determine whether *HER2* and *MYC* amplification status predicted clinical behaviour, we performed fluorescence *in situ* hybridization (FISH) for *HER2* and *MYC* on a cohort of 292 patients (Figure 5a), followed by survival analysis (Figure 5b). There were 272 cases for which *HER2* and *MYC* FISH was interpretable (Tables 1 and 2). Of these, 12.1% and 16.79% of cancers were *HER2* and *MYC* amplified, respectively. However, 29.2% of *MYC* amplifications occurred in the context of *HER2* amplification, suggesting selection for coamplification of *HER2* and *MYC*. We validated these findings using data from The Cancer Genome Atlas, which contains 821 breast cancer samples with available amplification status of both *HER2* and *MYC*, assessed by single-nucleotide polymorphism ChIP analysis (Supplementary Figure 3D).[43] Using the cBio data portal,[44] we determined that 12.4% (102/821) had *HER2* amplification and 13.5% (111/821) had *MYC* amplification. Further, of the *HER2*-amplified breast cancers, 19.6% (20/102) had *MYC* amplification, which corroborates our findings from the CREA cohort (Figure 5d). As expected from the

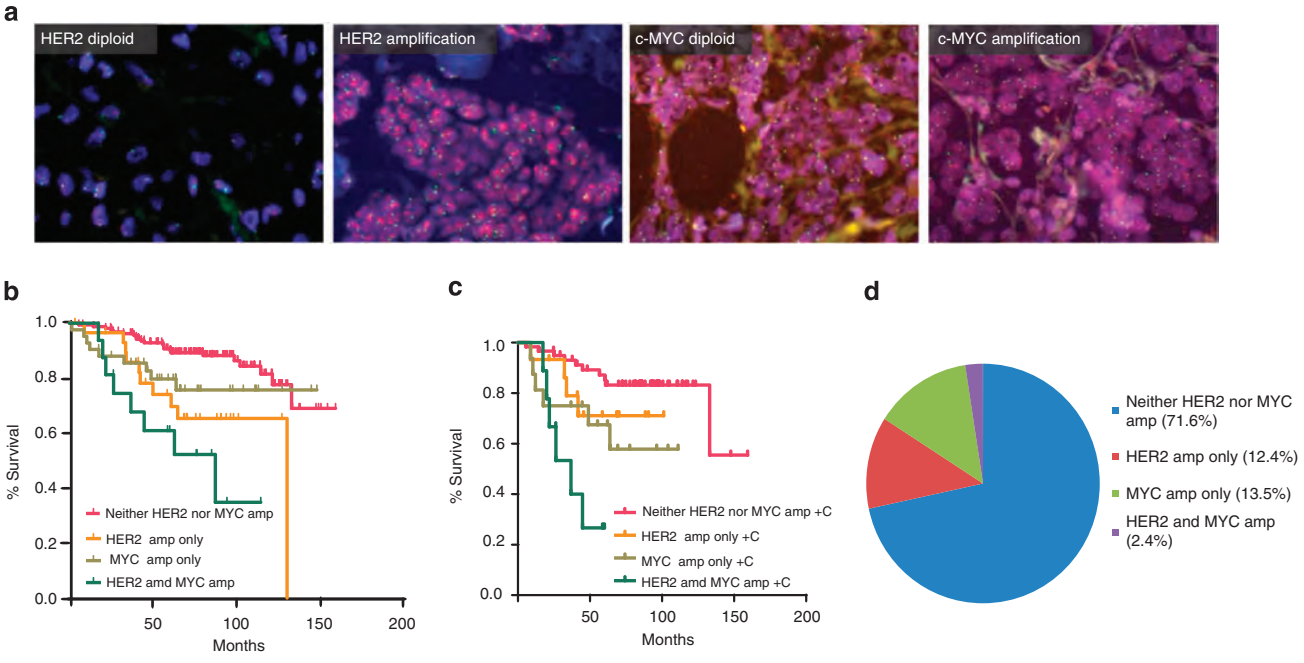

Figure 5. *HER2* and *MYC* amplification is associated with poor clinical outcome. (**a**) FISH was performed on 272 cases in the CREA cohort (see Materials and methods) to analyse *HER2* and *MYC* amplification status of patient tumours. (**b**) *MYC* amplification (HR 2.2) was weakly associated with breast cancer-specific death, with a lower HR than for *HER2* (HR 3.3). Coamplification of *HER2* and *MYC* was associated with a particularly poor prognosis (HR 3.8). (**c**) *HER2*- and *MYC*-coamplified cases respond poorly to chemotherapy. (**d**) Analysis of the The Cancer Genome Atlas cohort using the cBio data portal showed that 12.4% (102/821) had *HER2* amplification, 13.5% (111/821) had *MYC* amplification, 2.4% had coamplification of *HER2* and *MYC* (20/821; $P=0.06$, Fisher's exact test). Further, of the *HER2*-amplified breast cancers, 19.6% (20/102) have *MYC* amplification, which corroborates our findings from the CREA cohort.

Table 1. Clinicopathological associations of *c-Myc* and *Her2* coamplification

Clinicopathological parameter	*Total,* N = *279*	c-Myc *and* Her2 *amplified,* N = *17* *(6%)* (n *(%))*	*Not amplified,* N = *262* *(94%)* (n *(%))*	P-*value*[a]
Median (years) (range), 55 years (24–87)				0.62
Age ⩾ 55 years	129	9 (7%)	120 (93%)	
Age < 55 years	150	8 (5.3%)	142 (94.7%)	
Median size (mm) (range), 21 mm (0.9–80)				0.009
Size ⩾ 20 mm	110	12 (10.9%)	98 (89.1%)	
Size < 20 mm	169	5 (3.0%)	164 (7.0%)	
Grade				< 0.0001
3	126	17 (13%)	109 (87%)	
1 and 2	152	0 (0%)	152 (100%)	
Lymph node status				0.2
Lymph node positive	119	10 (8.4%)	109 (91.6%)	
Lymph node negative	157	7 (4.5%)	150 (95.5%)	
Oestrogen receptor				0.18
Positive	189	9 (4.8%)	180 (95.2%)	
Negative	86	8 (9.3%)	78 (90.7%)	
Progesterone receptor				0.07
Positive	158	6 (3.8%)	152 (96.2%)	
Negative	119	11 (9.2%)	108 (90.8%)	
Ki-67 > median				0.02
High	122	13 (10.7%)	109 (89.3%)	
Low	126	3 (2.4%)	123 (97.6%)	

[a] χ^2 analysis *P*-value.

Table 2. Univariate and multivariate analysis of clinicopathologic variables for breast cancer-specific death

Variable	*Hazards ratio (95% CI)*	P-*value*
(A) Univariate analysis		
Histological grade 3	3.5 (1.9–6.4)	< 0.0001
Size > 20 mm	2.5 (1.4–4.3)	0.002
Lymph nodes > 0	3.7 (2.0–6.7)	< 0.0001
ER positive	0.3 (0.2–0.5)	< 0.0001
PR positive	0.2 (0.1–0.3)	< 0.0001
Her2 amplified	3.5 (2.0–6.2)	< 0.0001
c-Myc amplified	2.2 (1.2–4.0)	0.01
Her2 and *c-Myc* coamplified	4.4 (2.0–9.5)	0.0002
(B) Multivariate analysis, resolved model		
Lymph nodes > 0	3.0 (1.6–5.6)	0.0004
PR positive	0.2 (0.1–0.4)	< 0.0001
Her2 and *c-Myc* coamplified	3.0 (1.4–6.5)	0.006

Abbreviations: CI, confidence interval; ER, oestrogen receptor; PR, progesterone receptor.

literature, *HER2* (hazard ratio (HR), 3.3; 95% confidence interval (CI): 1.8–5.8; $P = 0.001$) and *MYC* (HR, 2.2; 95% CI: 1.2–4.0; $P = 0.01$) amplification were significantly associated with a higher risk of breast cancer-specific death. However, there were 17 patients who showed coamplification of *HER2* and *MYC*, which was associated with a particularly poor prognosis (HR, 3.8; 95% CI: 1.8–8.2; $P = 0.006$) (Figure 5b). Coamplification of *HER2* and *MYC* was also associated with larger tumours, histological grade 3 and high Ki-67 expression. One of the phenotypes associated with CSCs is their inherent resistance to cytotoxic chemotherapy, which also contributes to relapse.[45,46] We analysed the outcome of a subgroup of patients who received adjuvant chemotherapy and found that patients with coamplification of *HER2* and *MYC* had a very poor outcome (Figure 5c). Using univariate analysis, coamplification of *HER2* and *MYC* was associated with an HR of 9.3 (95% CI: 2.04–42.3; $P = 0.004$) compared with amplification of *MYC* (HR, 3.8; 95% CI: 1.3–11.7; $P = 0.02$) or *HER2* (not significant). There have been conflicting reports on the association between *MYC* amplification in the context of *HER2* breast cancer patients and response to herceptin therapy.[47] We treated the Her2- and c-Myc-overexpressing cell lines with herceptin and assessed their self-renewal potential (Supplementary Figure 2F). The secondary tumoursphere-forming capacity of HM cells was robustly inhibited by herceptin treatment, suggesting that *HER2* patients with *MYC* amplification may still benefit from herceptin treatment.

DISCUSSION

Extensive heterogeneity exists at the inter- and intratumoral level in breast cancer.[48] There is increasing evidence that the tumourigenic and metastatic properties of some breast cancers are driven by subpopulations of cells (CSC) within the tumour with high self-renewal capacity.[36,49,50] We show here that cooperation of Her2 and c-Myc in malignancy promotes the formation of mammary tumours enriched with such cells. Earlier work[5] suggested that Her2 regulates the mammary stem/progenitor cell population, driving tumourigenesis and invasion. In addition, c-Myc has also been implicated in the generation or maintenance of physiological mammary stem cells and progenitor cells.[7] However, we have shown very modest effects of either oncogene alone on the tumour-propagating capacity and self-renewing phenotype compared with the large impact of coexpression of both oncogenes. Gene expression profiling for classification[20,21] revealed that the NM tumours clustered with claudin-low or basal-like mouse tumours and were enriched in the expression of mesenchymal genes (Figure 1C (b, e)). Several studies have alluded to the heterogeneous biology of HER2-overexpressing breast cancers.[51,52] The NM tumours (Supplementary Figure 1C) resemble the basal-HER2$^+$ breast cancers (oestrogen receptor-negative, HER2-positive and basal cytokeratin-positive), which constitute approximately 10% of HER2$^+$ breast cancers, and have poorer 5-year survival than basal-like breast cancers. The NM tumours generated might be a clinically relevant model in which we can test different treatment strategies in basal-HER2 breast cancers. In addition, array CGH analysis showed that NM tumours were more genomically unstable than N tumours, with a greater number of amplifications/deletions or rearrangements across multiple loci (Figure 1D and Supplementary Table T6), which may be related to the previously described role for c-Myc in genomic instability.[53] Coexpression of Her2/Neu and c-Myc (NM) was sufficient to significantly decrease survival time of mice (Figure 1B), increase self-renewal in sphere-forming assays (Figure 2b) and was associated with an average 20-fold increase of *in vivo* tumour-propagating capacity (Figure 2c), with some spontaneous tumours composed entirely of tumour-propagating capacities.

Strikingly, the acquisition of this phenotype is independent of a canonical EMT programme, which has been suggested to be intimately linked to the acquisition of a CSC phenotype[54]

(Figure 3c and Supplementary Figure 2D and E). This corroborates recent work[55] that the acquisition of an EMT programme by cancer cells can, in fact, suppress human tumour-initiating capability. The existence of epithelial tumour cell subpopulations that reversibly acquire a mesenchymal-like invasive state has been demonstrated in other models like prostate cancer.[55] Interestingly, in our model, HM cells express intermediate levels of both the epithelial and mesenchymal markers (Figure 3c). This observation was also supported by GSEA using representative EMT gene sets, suggesting that HM cells may transition between an epithelial and mesenchymal state.

In an effort to understand the molecular mechanisms by which Her2 and c-Myc cooperate, we used transcriptomics. Surprisingly, very few genes were dramatically regulated by coexpression of Her2 and c-Myc. One of these was LPL, an enzyme involved in triglyceride metabolism and cellular uptake,[56] which was strongly upregulated specifically in the HM cells. LPL has recently been reported as overexpressed in breast cancer[57] and subject to genomic translocations in squamous cell carcinoma.[58] GSEA analysis revealed global similarities between the transcriptome of HM cells and poor-prognosis B-CLL cells expressing high levels of LPL.[41,59] B-CLL is commonly associated with c-Myc overexpression,[60] and analysis of ENCODE[61] ChIP-Seq data revealed that c-Myc can bind to regions proximal to the LPL promoter in MCF10A cells, demonstrating the possibility of direct regulation by c-Myc (Supplementary Figure 3E). Knockdown of LPL in all the cell lines had a dramatic effect on the proliferative and tumoursphere-forming ability of cells, implying that LPL is important for their survival or self-renewal (Figure 4c,d). Interestingly, LPL is known to have a role in cholesterol metabolism and two gene sets involved in cholesterol biosynthesis and steroid metabolism were also significantly upregulated in the HM group (Figure 4b). LPL drives triglyceride hydrolysis in addition to fatty acid and lipoprotein uptake, which may act to create a fuel-rich niche for cancer cells.[62,63] On a broader scale, we observe a global quantitative increase in Myc-dependent transcription, rather than the acquisition of a novel repertoire of genes expressed. Whether these quantitative increases in the expression of many c-Myc targets contribute to the acquisition of a stem-like phenotype is unknown. However, we suggest that the function of c-Myc in cancer is dependent on the oncogenic milieu in which it is expressed (e.g., in the presence of *HER2* amplification) and that the function of c-Myc depends on certain thresholds of transcriptional activity. The importance of thresholds to Myc activity in cancer has previously been implicated in the induction of apoptosis by c-Myc.[64,65] Our work suggests that thresholds may similarly control other aspects of c-Myc function and resembles previous reports that embryonic stem cell self-renewal is associated with increased expression of many hundreds of Myc target genes.[23]

Our data demonstrate that only in the context of Her2 activation did c-Myc drive the acquisition of an aggressive stem-like phenotype, both *in vivo* (Figures 1 and 2) and *in vitro* (Figure 3). This may also help to explain why coamplification of *MYC* and *HER2* is overrepresented in breast cancers and portends very poor prognosis compared with the amplification of either oncogene alone (Figure 5). This may have important implications for the clinical management of *HER2*$^+$ patients. Further work is needed to determine whether *MYC* status defines *HER2*$^+$ breast cancers with fundamentally different biology or predicts response to cytotoxic chemotherapy or molecular targeted therapeutics such as herceptin and lapatinib.

MATERIALS AND METHODS

Preparation of primary MECs

Primary MECs from 8- to 12-week-old FVB/N recipient mice were cultured and retrovirally transduced as described previously[15,66] and allowed to attach overnight. MECs were retrovirally transduced with Neu14-pMIL and c-Myc (hs) pMig[15] transplanted into the cleared mammary fat pad of recipients.

Microarray experiments and mouse intrinsic gene set analysis

Microarrays of new samples were performed as previously described using custom Agilent 180K mouse microarrays (Agilent Technologies Inc., Santa Clara, CA, USA).[67] These arrays were normalized to samples from GSE3165 (22K), GSE27101 (44K) and GSE35722 (180K) using previously published methods.[67] Specifically, five C3-Tag and five mouse mammary tumour virus-Neu tumours from each of the three platforms (30 microarrays total) were used to calculate a median normalization factor for common probes across all three platforms. Supervised clustering was performed using the 2007 intrinsic probe list.[20] Of the 866 original probes, 655 were found on all three array platforms used.

Copy number variation analysis by array CGH

DNA was extracted from snap frozen mammary tumour and liver (reference from sex-matched wild-type FVB/N mouse) using the QIAamp DNA Mini Kit (Qiagen, Doncaster, VIC, Australia) according to the manufacturer's instructions. Array CGH was performed by the Ramaciotti Centre for Gene Function Analysis (Randwick, Sydney, NSW, Australia) on differentially labelled tumour DNA (Cy5) and sex-matched reference liver DNA (Cy3) using the Agilent SurePrint G3 mouse CGH 4×180K microarray platform. The array CGH data were analysed using circular binary segmentation[68] to translate intensity measurements into regions of equal copy number. Analysis was carried out using the DNAcopy package (http: //www.bioconductor.org/) in R2.15.2 (http: //www.r-project.org/).

Preparation of tumours

Tumour cells were prepared as described before[69] and resuspended in the MEC medium.

Tumoursphere assay

Dissociated cells from tumours or modified MCF10A cell lines were put into the tumoursphere assay as described previously.[36] Herceptin was added at a concentration of 21 μg/ml to assay for the effect of herceptin on self-renewal.

Flow cytometry

Tumours were processed into single-cell suspensions before staining and fluorescence-activated cell sorting (FACS) as described previously[69] (Table 3). Flow cytometry was performed on a BD LSRII SORP using the FACS DIVA software (BD Biosciences, San Jose, CA, USA), and data were analysed using the FlowJo software (Treestar, Ashland, OR, USA).

Immunohistochemistry

Full details of the protocols for immunohistochemistry are shown in Supplementary Table T2. Intrinsic breast cancer subtypes were assessed immunohistochemically using criteria similar to those recently described by Cheang and co-workers,[70] but using FISH to determine HER2 status. The details of antibodies, immunohistochemistry, *in situ* hybridization and scoring for these markers have been previously reported in the invasive ductal carcinoma cohort.[69]

Limiting dilution assay

Single-cell suspensions of viable tumour cells were prepared as described before in the Materials and methods section. Tumour cells were transplanted in appropriate numbers into the fourth mammary fat pad of 8- to 12-week-old syngeneic mice and aged till ethical end point. Extreme limiting dilution analysis[71] software was used to calculate the TPF.

Cell lines

MCF10A EcoR cells[72] were cultured as per ATCC guidelines. Her2WT pMihR- and c-Myc pMig-modified cell lines were created by retroviral transduction of the cells with the appropriate retroviral supernatants. The stable cells lines generated were checked for Her2 and c-Myc overexpression by western blots and quantitative PCR.

Table 3. Antibodies used in FACS analysis

Antibody	*Dilution*	*Company, Clone*
Mouse		
Anti-CD16/CD32	1:200	BD Biosciences (BD Australia, North Ryde, NSW, Australia), Clone: 2.4G2
Anti-CD31-biotin	1:40	BD Biosciences, Clone: 390
Anti-CD45-biotin	1:100	BD Biosciences, Clone:30-F11
Anti-TER119-biotin	1:80	BD Biosciences, Clone: TER119
Anti-BP-biotin	1:50	eBiosciences, (Jomar Bioscience, Kensington, SA, Australia) Clone: 6C3
Streptavidin-APC-Cy7	1:400	BD Biosciences
Anti-CD24-PE-Cy7	1:400	BD Biosciences, Clone: M1/69
Anti-CD29-Pacific Blue	1:100	BioLegend (San Diego, CA, USA), Clone: HMb1-1
Anti-CD61-APC	1:100	Invitrogen, Clone: HMb1-1
Human		
Anti-CD24-AlexaFluor647	1:20	BD Biosciences, Clone: ML5
Anti-EpCAM-PerCP-Cy5.5	1:10	BD Biosciences, Clone: EBA-1
Anti-CD44-biotin	1:40	BD Biosciences, Clone: G44-26
Streptavidin-APC-Cy7	1:400	BD Biosciences

Abbreviation: FACS, fluorescence-activated cell sorting.

LPL knockdown

pMisssion shLPL constructs (Sigma Aldrich, Castle Hill, NSW, Australia) TRCN0000052142 sequence, 5′-CCGGGCTCTGCTTGAGTTGTAGAAACTCGAGT TTCTACAACTCAAGCAGAGCTTTTTG-3′ and appropriate controls were used to generate V, H, M and HM cell lines with LPL knockdown. Live cultures were analysed using time-lapse phase-contrast microscopy at 37 °C with the automated Live Cell Imaging System IncuCyte zoom40061 FLR (Essen Bioscience Inc., Ann Arbor, MI, USA). A total of 2×10^4 cells per well were seeded triplicate in a 24-well plate, which was immediately loaded into the IncuCyte imaging system. Nine images per well were collected at 2 h intervals. The percent confluence of the live cultures was calculated using the IncuCyte software (Essen Bioscience Inc.). Briefly, average confluence was calculated using individual data from each of the nine images taken per well at each time point. The data points represent the mean of three wells (± s.e.m.). Data analysis was completed using Prism (GraphPad Software, La Jolla, CA, USA).

MTS assay

Cell viability assay (MTS assay) was carried out using the CellTiter 96 AQueous Cell Proliferation Assay (G5421; Promega, Alexandria, NSW, Australia) according to the manufacturer's recommendation.

Western blots

Protein lysates were run on sodium dodecyl sulfate–polyacrylamide gel electrophoresis gels following transfer to 0.45 μm polyvinylidene difluoride membranes as described previously using standard procedures.[66] The membranes were incubated with primary antibody solutions at concentration according to Supplementary Table T3.

Quantitative real-time PCR

cDNA was generated from 500 ng of RNA using the Superscript III first-strand synthesis system (Invitrogen, Mulgrave, VIC, Australia) according to the manufacturer's protocol. Quantitative real-time PCR was carried out using the Roche Universal ProbeLibrary System (Roche Diagnostics, Castle Hill, NSW, Australia) on the Roche LightCycler480 (see Supplementary Table T5) as per the manufacturer's instructions, using primers as shown in Supplementary Table T4.

Transcript profiling

Total RNA was extracted by using the Qiagen RNeasy minikit (Qiagen, Doncaster, VIC, Australia) according to the manufacturer's protocol. mRNA expression profiling was performed by the Ramaciotti Centre for Gene Function Analysis (Kensington, NSW, Australia) using the Affymetrix GeneChip Gene 1.0 ST Array (Affymetrix, Santa Clara, CA, USA). Because of one of our Myc-overexpressing samples failing quality control, we removed this from the microarray analysis. Normalization and probe set summarization was performed using the robust multichip average[73] implemented in the Affy library[74] from R.[75] Control probe sets were removed leaving 28 869 probe sets on the array. Differential gene expression was then assessed for each probe set using an empirical Bayes, moderated t-statistic implemented in Limma[76] using the limmaGP tool in GenePattern. GSEA[39] was run with the GenePattern tool GSEApreranked using a ranked list of the Limma moderated t-statistics against version 3.0 of the 'C2_all' curated gene sets from the MSigDB.[39] All analyses were performed using GenePattern software[77] and are available at http://pwbc.garvan.unsw.edu.au/gp/. Microarray data are available from GEO: GSE43730.

Patients

The Garvan/St Vincent's Hospital outcome series comprises 292 operable invasive ductal carcinomas of the breast from patients treated by a single surgeon between February 1992 and August 2002 at St Vincent's Hospital, Sydney, NSW, Australia. Ethics approval was granted for the use of pathology specimens and cognate clinicopathological data (Human Research Ethics Committee of St Vincent's Hospital, Sydney, NSW, Australia). A more detailed description of the clinicopathological characteristics of the cohort is published elsewhere.[78–80]

Fluorescence *in situ* hybridization

HER2 FISH was performed by Dr Adrienne Morey and co-workers[81] in the *HER2* FISH Reference Lab at St Vincent's Hospital, according to routine protocols used for diagnostic cases. *HER2* gene amplification was defined as a *HER2*/chr17 ratio >2.2. *MYC* ISH was performed using similar methods, but using the Vysis *MYC/CEP8* probe. A minimum of 20 cells for each tumour was counted by a specialist breast pathologist (SO'T). A mean score for *MYC*, *CEP8* and the *MYC/CEP8* ratio was calculated. Using the criteria of Perez *et al.*,[82] an *MYC/CEP8* ratio of >1.3 or a mean tumour cell *MYC* copy number of >5 was used to determine cases with *MYC* amplification.

Statistical analysis

Statistical evaluation was performed using Statview 5.0 Software (Abacus Systems, Berkeley, CA, USA). A *P*-value of <0.05 was accepted as statistically significant.

CONFLICT OF INTEREST

The authors declare no conflict of interest.

ACKNOWLEDGEMENTS

We thank Professor JM Bishop and The GW Hooper Foundation (UCSF); Nikki Ailing and Alice Boulghourjian for technical assistance with Flow cytometry and Immunohistochemistry, respectively; and Aurelie Cazet for proof reading the manuscript. WST is a recipient of an International Postgraduate Research Scholarship (IPRS) and the Beth Yarrow Memorial Award in Medical Science. We would like to acknowledge funding from Victoria Taylor, Sydney Breast Cancer Foundation, CCNSW and Colin Biggers & Paisley, Sydney. This research was supported by an Early Career Fellowship from the National Breast Cancer Foundation Australia. AS is a Career Development Fellow of the National Health and Medical Research Council of Australia. SOT is funded by the Cancer Institute NSW Clinical Research Fellowship 10-CRF 1-07.

REFERENCES

1 Jemal A, Siegel R, Xu J, Ward E. Cancer statistics, 2010. *CA Cancer J Clin* 2010; **60**: 277–300.
2 Slamon DJ, Godolphin W, Jones LA, Holt JA, Wong SG, Keith DE *et al.* Studies of the HER-2/neu proto-oncogene in human breast and ovarian cancer. *Science* 1989; **244**: 707–712.
3 Moasser MM. The oncogene HER2: its signaling and transforming functions and its role in human cancer pathogenesis. *Oncogene* 2007; **26**: 6469–6487.
4 Magnifico A, Albano L, Campaner S, Delia D, Castiglioni F, Gasparini P *et al.* Tumor-initiating cells of HER2-positive carcinoma cell lines express the highest

oncoprotein levels and are sensitive to trastuzumab. *Clin Cancer Res* 2009; **15**: 2010–2021.
5 Korkaya H, Paulson A, Iovino F, Wicha MS. HER2 regulates the mammary stem/progenitor cell population driving tumorigenesis and invasion. *Oncogene* 2008; **27**: 6120–6130.
6 Fernandez PC, Frank SR, Wang L, Schroeder M, Liu S, Greene J *et al.* Genomic targets of the human c-Myc protein. *Genes Dev* 2003; **17**: 1115–1129.
7 Stoelzle T, Schwarb P, Trumpp A, Hynes NE. c-Myc affects mRNA translation, cell proliferation and progenitor cell function in the mammary gland. *BMC Biol* 2009; **7**: 63.
8 Takahashi K, Yamanaka S. Induction of pluripotent stem cells from mouse embryonic and adult fibroblast cultures by defined factors. *Cell* 2006; **126**: 663–676.
9 Wong DJ, Liu H, Ridky TW, Cassarino D, Segal E, Chang HY. Module map of stem cell genes guides creation of epithelial cancer stem cells. *Cell Stem Cell* 2008; **2**: 333–344.
10 Deming SL, Nass SJ, Dickson RB, Trock BJ. C-myc amplification in breast cancer: a meta-analysis of its occurrence and prognostic relevance. *Br J Cancer* 2000; **83**: 1688–1695.
11 Persons DL, Borelli KA, Hsu PH. Quantitation of HER-2/neu and c-myc gene amplification in breast carcinoma using fluorescence *in situ* hybridization. *Mod Pathol* 1997; **10**: 720–727.
12 Park K, Kwak K, Kim J, Lim S, Han S. c-myc amplification is associated with HER2 amplification and closely linked with cell proliferation in tissue microarray of nonselected breast cancers. *Hum Pathol* 2005; **36**: 634–639.
13 Hynes NE, Lane HA. Myc and mammary cancer: Myc is a downstream effector of the ErbB2 receptor tyrosine kinase. *J Mamm Gland Biol Neoplasia* 2001; **6**: 141–150.
14 Neve RM, Chin K, Fridlyand J, Yeh J, Baehner FL, Fevr T *et al.* A collection of breast cancer cell lines for the study of functionally distinct cancer subtypes. *Cancer Cell* 2006; **10**: 515–527.
15 Welm AL, Kim S, Welm BE, Bishop JM. MET and MYC cooperate in mammary tumorigenesis. *Proc Natl Acad Sci USA* 2005; **102**: 4324–4329.
16 Stewart TA, Pattengale PK, Leder P. Spontaneous mammary adenocarcinomas in transgenic mice that carry and express MTV/myc fusion genes. *Cell* 1984; **38**: 627–637.
17 D'Cruz CM, Gunther EJ, Boxer RB, Hartman JL, Sintasath L, Moody SE *et al.* c-MYC induces mammary tumorigenesis by means of a preferred pathway involving spontaneous Kras2 mutations. *Nat Med* 2001; **7**: 235–239.
18 Bargmann CI, Weinberg RA. Increased tyrosine kinase activity associated with the protein encoded by the activated neu oncogene. *Proc Natl Acad Sci USA* 1988; **85**: 5394–5398.
19 Guy CT, Webster MA, Schaller M, Parsons TJ, Cardiff RD, Muller WJ. Expression of the neu protooncogene in the mammary epithelium of transgenic mice induces metastatic disease. *Proc Natl Acad Sci USA* 1992; **89**: 10578–10582.
20 Herschkowitz JI, Simin K, Weigman VJ, Mikaelian I, Usary J, Hu Z *et al.* Identification of conserved gene expression features between murine mammary carcinoma models and human breast tumors. *Genome Biol* 2007; **8**: R76.
21 Herschkowitz JI, Zhao W, Zhang M, Usary J, Murrow G, Edwards D *et al.* Comparative oncogenomics identifies breast tumors enriched in functional tumor-initiating cells. *Proc Natl Acad Sci* 2011; **109**: 2778–2783.
22 Muller WJ, Sinn E, Pattengale PK, Wallace R, Leder P. Single-step induction of mammary adenocarcinoma in transgenic mice bearing the activated c-neu oncogene. *Cell* 1988; **54**: 105–115.
23 Kim J, Woo AJ, Chu J, Snow JW, Fujiwara Y, Kim CG *et al.* A Myc network accounts for similarities between embryonic stem and cancer cell transcription programs. *Cell* 2010; **143**: 313–324.
24 Wolfer A, Wittner BS, Irimia D, Flavin RJ, Lupien M, Gunawardane RN *et al.* MYC regulation of a 'poor-prognosis' metastatic cancer cell state. *Proc Natl Acad Sci* 2010; **107**: 3698–3703.
25 Lo PK, Kanojia D, Liu X, Singh UP, Berger FG, Wang Q *et al.* CD49f and CD61 identify Her2/neu-induced mammary tumor-initiating cells that are potentially derived from luminal progenitors and maintained by the integrin-TGF[beta] signaling. *Oncogene* 2011; **31**: 2614–2626.
26 Liu JC, Deng T, Lehal RS, Kim J, Zacksenhaus E. Identification of tumorsphere- and tumor-initiating cells in HER2/Neu-induced mammary tumors. *Cancer Res* 2007; **67**: 8671–8681.
27 Lee T, Yao G, Nevins J, You L. Sensing and integration of Erk and PI3K signals by Myc. *PLoS Comput Biol* 2008; **4**: e1000013.
28 Sears R, Nuckolls F, Haura E, Taya Y, Tamai K, Nevins JR. Multiple Ras-dependent phosphorylation pathways regulate Myc protein stability. *Genes Dev* 2000; **14**: 2501–2514.
29 Hardy KM, Booth BW, Hendrix MJ, Salomon DS, Strizzi L. ErbB/EGF signaling and EMT in mammary development and breast cancer. *J Mammary Gland Biol Neoplasia* 2010; **15**: 191–199.
30 Gregory PA, Bert AG, Paterson EL, Barry SC, Tsykin A, Farshid G *et al.* The miR-200 family and miR-205 regulate epithelial to mesenchymal transition by targeting ZEB1 and SIP1. *Nat Cell Biol* 2008; **10**: 593–601.
31 Dykxhoorn DM, Wu Y, Xie H, Yu F, Lal A, Petrocca F *et al.* MiR-200 enhances mouse breast cancer cell colonization to form distant metastases. *PLoS One* 2009; **4**: e7181.
32 Sarrio D, Rodriguez-Pinilla SM, Hardisson D, Cano A, Moreno-Bueno G, Palacios J. Epithelial–mesenchymal transition in breast cancer relates to the basal-like phenotype. *Cancer Res* 2008; **68**: 989–997.
33 Alonso SR, Tracey L, Ortiz P, Perez-Gomez B, Palacios J, Pollan M *et al.* A high-throughput study in melanoma identifies epithelial–mesenchymal transition as a major determinant of metastasis. *Cancer Res* 2007; **67**: 3450–3460.
34 Gupta PB, Fillmore CM, Jiang G, Shapira SD, Tao K, Kuperwasser C *et al.* Stochastic state transitions give rise to phenotypic equilibrium in populations of cancer cells. *Cell* 2011; **146**: 633–644.
35 Fillmore CM, Kuperwasser C. Human breast cancer cell lines contain stem-like cells that self-renew, give rise to phenotypically diverse progeny and survive chemotherapy. *Breast Cancer Res* 2008; **10**: R25.
36 Al-Hajj M, Wicha MS, Benito-Hernandez A, Morrison SJ, Clarke MF. Prospective identification of tumorigenic breast cancer cells. *Proc Natl Acad Sci USA* 2003; **100**: 3983–3988.
37 Visvader JE, Lindeman GJ. Cancer stem cells in solid tumours: accumulating evidence and unresolved questions. *Nat Rev Cancer* 2008; **8**: 755–768.
38 Vaillant F, Asselin-Labat ML, Shackleton M, Forrest NC, Lindeman GJ, Visvader JE. The mammary progenitor marker CD61/beta3 integrin identifies cancer stem cells in mouse models of mammary tumorigenesis. *Cancer Res* 2008; **68**: 7711–7717.
39 Subramanian A, Tamayo P, Mootha VK, Mukherjee S, Ebert BL, Gillette MA *et al.* Gene set enrichment analysis: a knowledge-based approach for interpreting genome-wide expression profiles. *Proc Natl Acad Sci USA* 2005; **102**: 15545–15550.
40 Matthews L, Gopinath G, Gillespie M, Caudy M, Croft D, de Bono B *et al.* Reactome knowledgebase of human biological pathways and processes. *Nucleic Acids Res* 2009; **37**(Suppl 1): D619–D622.
41 Bilban M, Heintel D, Scharl T, Woelfel T, Auer MM, Porpaczy E *et al.* Deregulated expression of fat and muscle genes in B-cell chronic lymphocytic leukemia with high lipoprotein lipase expression. *Leukemia* 2006; **20**: 1080–1088.
42 Kim YH, Girard L, Giacomini CP, Wang P, Hernandez-Boussard T, Tibshirani R *et al.* Combined microarray analysis of small cell lung cancer reveals altered apoptotic balance and distinct expression signatures of MYC family gene amplification. *Oncogene* 2005; **25**: 130–138.
43 Cancer Genome Atlas Network. Comprehensive molecular portraits of human breast tumours. *Nature* 2012; **490**: 61–70.
44 Cerami E, Gao J, Dogrusoz U, Gross BE, Sumer SO, Aksoy BA *et al.* The cBio Cancer Genomics Portal: an open platform for exploring multidimensional cancer genomics data. *Cancer Discov* 2012; **2**: 401–404.
45 Wicha MS, Liu S, Dontu G. Cancer stem cells: an old idea—a paradigm shift. *Cancer Res* 2006; **66**: 1883–1890.
46 Ginestier C, Liu S, Diebel ME, Korkaya H, Luo M, Brown M *et al.* CXCR1 blockade selectively targets human breast cancer stem cells *in vitro* and in xenografts. *J Clin Invest* 2010; **120**: 485–497.
47 Perez EA, Jenkins RB, Dueck AC, Wiktor AE, Bedroske PP, Anderson SK *et al.* C-MYC alterations and association with patient outcome in early-stage HER2-positive breast cancer from the north central cancer treatment group N9831 adjuvant trastuzumab trial. *J Clin Oncol* 2011; **29**: 651–659.
48 Axelrod R, Axelrod DE, Pienta KJ.. Evolution of cooperation among tumor cells. *Proc Natl Acad Sci USA* 2006; **103**: 13474–13479.
49 Lapidot T, Sirard C, Vormoor J, Murdoch B, Hoang T, Caceres-Cortes J *et al.* A cell initiating human acute myeloid leukaemia after transplantation into SCID mice. *Nature* 1994; **367**: 645–648.
50 Singh SK, Clarke ID, Terasaki M, Bonn VE, Hawkins C, Squire J *et al.* Identification of a cancer stem cell in human brain tumors. *Cancer Res* 2003; **63**: 5821–5828.
51 Liu H, Fan QH, Zhang ZH, Li X, Yu HP, Meng FQ. Basal-HER2 phenotype shows poorer survival than basal-like phenotype in hormone receptor-negative invasive breast cancers. *Hum Pathol* 2008; **39**: 167–174.
52 Bagaria SP, Ray PS, Wang J, Kropcho L, Chung A, Sim MS *et al.* Prognostic value of basal phenotype in HER2-overexpressing breast cancer. *Ann Surg Oncol* 2012; **19**: 935–940.
53 Felsher DW, Bishop JM. Transient excess of MYC activity can elicit genomic instability and tumorigenesis. *Proc Natl Acad Sci USA* 1999; **96**: 3940–3944.
54 Thiery JP, Acloque H, Huang RY, Nieto MA. Epithelial-mesenchymal transitions in development and disease. *Cell* 2009; **139**: 871–890.
55 Celià-Terrassa T, Meca-Cortés Ó, Mateo F, Martínez de Paz A, Rubio N, Arnal-Estapé A *et al.* Epithelial–mesenchymal transition can suppress major attributes of human epithelial tumor-initiating cells. *J Clin Invest* 2012; **122**: 1849–1868.
56 Mead JR, Irvine SA, Ramji DP. Lipoprotein lipase: structure, function, regulation, and role in disease. *J Mol Med* 2002; **80**: 753–769.

57 Prat A, Parker JS, Karginova O, Fan C, Livasy C, Herschkowitz JI *et al.* Phenotypic and molecular characterization of the claudin-low intrinsic subtype of breast cancer. *Breast Cancer Res* 2010; **12**: R68.
58 Carter SA, Foster NA, Scarpini CG, Chattopadhyay A, Pett MR, Roberts I *et al.* Lipoprotein lipase is frequently overexpressed or translocated in cervical squamous cell carcinoma and promotes invasiveness through the non-catalytic C terminus. *Br J Cancer* 2012; **107**: 739–747.
59 Heintel D, Kienle D, Shehata M, Krober A, Kroemer E, Schwarzinger I *et al.* High expression of lipoprotein lipase in poor risk B-cell chronic lymphocytic leukemia. *Leukemia* 2005; **19**: 1216–1223.
60 Zhang W, Kater AP, Widhopf GF, Chuang H-Y, Enzler T, James DF *et al.* B-cell activating factor and v-Myc myelocytomatosis viral oncogene homolog (c-Myc) influence progression of chronic lymphocytic leukemia. *Proc Natl Acad Sci* 2010; **107**: 18956–18960.
61 Rosenbloom KR, Sloan CA, Malladi VS, Dreszer TR, Learned K, Kirkup VM *et al.* ENCODE Data in the UCSC Genome Browser: year 5 update. *Nucleic Acids Res* 2013; **41**: D56–D63.
62 Danilo C, Frank PG. Cholesterol and breast cancer development. *Curr Opin Pharmacol* 2012; **12**: 677–682.
63 Llaverias G, Danilo C, Mercier I, Daumer K, Capozza F, Williams TM *et al.* Role of cholesterol in the development and progression of breast cancer. *Am J Pathol* 2011; **178**: 402–412.
64 Shachaf CM, Gentles AJ, Elchuri S, Sahoo D, Soen Y, Sharpe O *et al.* Genomic and proteomic analysis reveals a threshold level of MYC required for tumor maintenance. *Cancer Res* 2008; **68**: 5132–5142.
65 Murphy DJ, Junttila MR, Pouyet L, Karnezis A, Shchors K, Bui DA *et al.* Distinct thresholds govern Myc's biological output *in vivo*. *Cancer Cell* 2008; **14**: 447–457.
66 Swarbrick A, Roy E, Allen T, Bishop JM. Id1 cooperates with oncogenic Ras to induce metastatic mammary carcinoma by subversion of the cellular senescence response. *Proc Natl Acad Sci USA* 2008; **105**: 5402–5407.
67 Roberts PJ, Usary JE, Darr DB, Dillon PM, Pfefferle AD, Whittle MC *et al.* Combined PI3K/mTOR and MEK inhibition provides broad antitumor activity in faithful murine cancer models. *Clin Cancer Res* 2012; **18**: 5290–5303.
68 Olshen AB, Venkatraman ES, Lucito R, Wigler M. Circular binary segmentation for the analysis of array-based DNA copy number data. *Biostatistics* 2004; **5**: 557–572.
69 O'Toole SA, Machalek DA, Shearer RF, Millar EKA, Nair R, Schofield P *et al.* Hedgehog overexpression is associated with stromal interactions and predicts for poor outcome in breast cancer. *Cancer Res* 2011; **71**: 4002–4014.
70 Cheang MC, Voduc D, Bajdik C, Leung S, McKinney S, Chia SK *et al.* Basal-like breast cancer defined by five biomarkers has superior prognostic value than triple-negative phenotype. *Clin Cancer Res* 2008; **14**: 1368–1376.
71 Hu Y, Smyth GK. ELDA: extreme limiting dilution analysis for comparing depleted and enriched populations in stem cell and other assays. *J Immunol Methods* 2009; **347**: 70–78.
72 Brummer T, Schramek D, Hayes VM, Bennett HL, Caldon CE, Musgrove EA *et al.* Increased proliferation and altered growth factor dependence of human mammary epithelial cells overexpressing the Gab2 docking protein. *J Biol Chem* 2006; **281**: 626–637.
73 Irizarry RA, Bolstad BM, Collin F, Cope LM, Hobbs B, Speed TP. Summaries of Affymetrix GeneChip probe level data. *Nucleic Acids Res* 2003; **31**: e15.
74 Gautier L, Cope L, Bolstad BM, Irizarry RA. affy—analysis of Affymetrix GeneChip data at the probe level. *Bioinformatics* 2004; **20**: 307–315.
75 Gentleman RC, Carey VJ, Bates DM, Bolstad B, Dettling M, Dudoit S *et al.* Bioconductor: open software development for computational biology and bioinformatics. *Genome Biol* 2004; **5**: R80.
76 Smyth GK. Linear models and empirical bayes methods for assessing differential expression in microarray experiments. *Stat Appl Genet Mol Biol* 2004; **3**: (Article 3).
77 Reich M, Liefeld T, Gould J, Lerner J, Tamayo P, Mesirov JP. GenePattern 2.0. *Nat Genet* 2006; **38**: 500–501.
78 Lopez-Knowles E, O'Toole SA, McNeil CM, Millar EK, Qiu MR, Crea P *et al.* PI3K pathway activation in breast cancer is associated with the basal-like phenotype and cancer-specific mortality. *Int J Cancer* 2010; **126**: 1121–1131.
79 Lopez-Knowles E, Zardawi SJ, McNeil CM, Millar EK, Crea P, Musgrove EA *et al.* Cytoplasmic localization of beta-catenin is a marker of poor outcome in breast cancer patients. *Cancer Epidemiol Biomarkers Prev* 2010; **19**: 301–309.
80 Millar EK, Anderson LR, McNeil CM, O'Toole SA, Pinese M, Crea P *et al.* BAG-1 predicts patient outcome and tamoxifen responsiveness in ER-positive invasive ductal carcinoma of the breast. *Br J Cancer* 2009; **100**: 123–133.
81 Laudadio J, Quigley DI, Tubbs R, Wolff DJ. HER2 testing: a review of detection methodologies and their clinical performance. *Expert Rev Mol Diagn* 2007; **7**: 53–64.
82 Perez E, Reinholz M, Dueck A, Wiktor A, Lingle W, Davidson N *et al.* c-MYC amplification and correlation with patient outcome in early stage HER2+ breast cancer from the NCCTG adjuvant intergroup trial N9831. *Cancer Res* 2009; **69**(Suppl): 56.

Supplementary Information accompanies this paper on the Oncogene website (http://www.nature.com/onc)